



ELSEVIER

Journal of Power Sources 95 (2001) 203–208

JOURNAL OF
POWER
SOURCES

www.elsevier.com/locate/jpowsour

In situ observation of morphology change in lead dioxide surface for lead-acid battery

Masashi Shiota^{a,*}, Yoshiaki Yamaguchi^{a,c}, Yasuhide Nakayama^a, Kazuyuki Adachi^b,
Shunji Taniguchi^b, Nobumitsu Hirai^c, Shigeta Hara^c

^aYuasa Corporation, 2-3-21 Kosobe-cho, Takatsuki, Osaka 569-1115, Japan

^bKyusyu Electric Power Co. Inc., 2-1-47 Shiobaru, Minami-ku, Fukuoka 815-0032, Japan

^cDepartment of Materials Science & Processing, Graduate School of Engineering, Osaka University, 2-1 Yamadaoka, Suita, Osaka 565-0871, Japan

Abstract

An electrochemical atomic force microscope (EC-AFM) was used to study the reaction of a lead dioxide electrode in sulfuric acid solution, while the reaction corresponding to what occurs at the positive electrode of a lead-acid battery took place. We observed continuous in situ morphology change of the lead dioxide electrode and the potentiostatic transient, when the oxidation and reduction potentials were applied to the electrode. As a result, it was confirmed that lead sulfate crystals began to deposit from the moment when the reduction potential was applied and the reduction transient showed a sharp peak shape at the same time. On the other hand, the dissolution of lead sulfate crystals was delayed from the moment when the oxidation potential was applied. It took about 2 min for all the crystals to dissolve, and the oxidation transient was recorded as a broad shaped curve. © 2001 Published by Elsevier Science B.V.

Keywords: In situ observation; EC-AFM; Potentiostatic transient; Lead-acid battery; Lead dioxide electrodes

1. Introduction

We are now using an electrochemical atomic force microscope (EC-AFM) as a new analysis technique for the detailed understanding of the reaction processes in lead-acid batteries, because the AFM can make in situ observation of the electrode surface morphology and its change. In the previous investigation, we succeeded in observing the in situ morphology change of a lead electrode in sulfuric acid during oxidation and reduction, as a model of the negative electrode reaction [1,2]. This successful observation result is useful for designing a low cost battery for HEV, EV and other novel applications with the improvement of the specific power and the charge acceptability of the negative electrode in the lead-acid battery [3,4].

It is, however, also important for achievement of higher battery performance to study positive electrode behavior. Premature capacity loss (PCL), Sb free effect, active material utilization and corrosion resistance of the grid in a positive electrode are major issues that have to be solved by more detailed analysis [5–11].

Therefore, we have started to study the electrochemical reaction of a lead dioxide electrode using the in situ EC-AFM technique. As the first trial, we investigated the morphology change of the lead dioxide electrode by EC-AFM and the potentiostatic transient when the oxidation and reduction potentials were applied. As a result, we observed an interesting behavior of the lead dioxide electrode in oxidation/reduction cycle, which was obviously different from the behavior of the lead electrode.

2. Experimental

2.1. EC-AFM equipment

In this study, we used an EC-AFM unit made by Molecular Imaging (MI) Co. with a control unit made by Digital Instruments (DI) Co. (model NanoScope IIIa) for in situ observation of the electrochemical reaction, $\text{PbO}_2 + \text{H}_2\text{SO}_4 + 2\text{H}^+ + 2\text{e}^- \rightleftharpoons \text{PbSO}_4 + 2\text{H}_2\text{O}$. The AFM experiments were performed utilizing a commercial Si_3N_4 cantilever with integral Au coated tips, a PbO_2 electrode as a counter and a $\text{Hg}/\text{Hg}_2\text{SO}_4$ electrode as a reference for the electrochemical cell. All potentials reported here are referred to this electrode. The electrochemical operations in this experiment were carried out by using a potentiostat.

* Corresponding author. Tel.: +81-726-85-2682; fax: +81-726-85-3070.
E-mail address: masashi_shiota@yuasa-jpn.co.jp (M. Shiota).

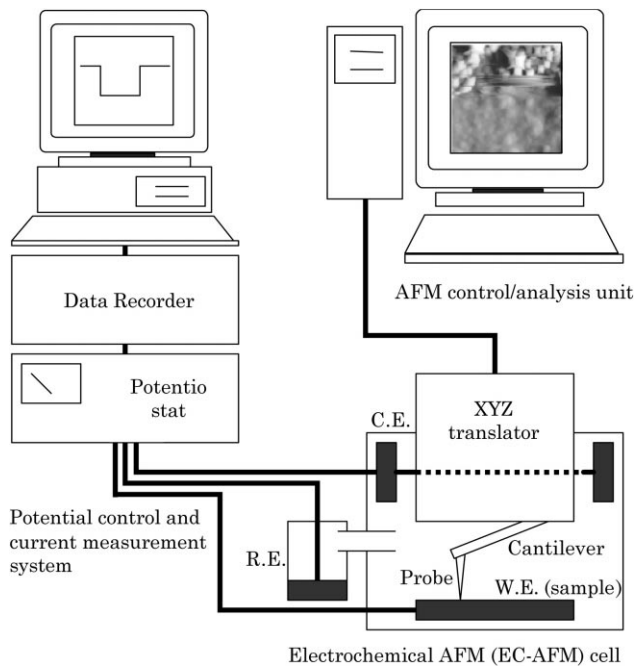


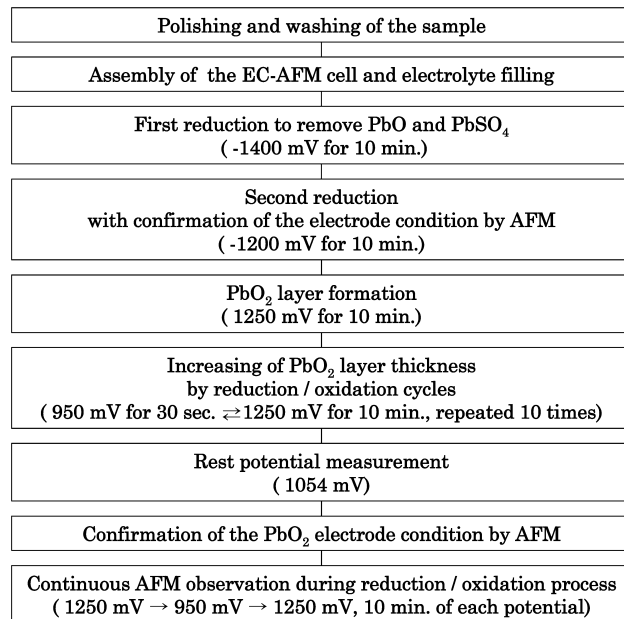
Fig. 1. Schematic experimental set-up of the EC-AFM equipment: W.E. is a sample electrode; C.E. is PbO_2 counter electrode; R.E. is $\text{Hg}/\text{Hg}_2\text{SO}_4$ reference electrode.

galvano stat (model HA-151) made by Hokuto Denko Co. A schematic experimental set-up of this EC-AFM equipment is shown in Fig. 1.

2.2. Sample electrode preparation

Before the EC-AFM experiments, the cell was assembled and the lead dioxide electrode was prepared in the EC-AFM cell as a working electrode.

The surface of a pure lead sheet sample (99.99%) was first polished and washed with ethanol, and then the sample was assembled into the cell. The EC-AFM cell was filled with $1.250 \text{ g}/\text{cm}^3$ sulfuric acid electrolyte and two-step potentials were applied to remove completely the lead oxide and lead sulfate on the sample electrode surface at -1400 and -1200 mV. Each reduction potential was maintained for 10 min by the potentiostat. It was confirmed by AFM observation that no lead sulfate existed on the sample surface at the second reduction step. After that, the sample electrode was oxidized at 1250 mV for 10 min to form a lead dioxide layer on the lead substrate. To increase the layer thickness, the potentiostatic reduction/oxidation cycles were repeated 10 times. The reduction and oxidation conditions used in this electrode preparation cycle were 950 mV for 30 s and 1250 mV for 10 min, respectively. The potential of the electrode was then measured, and this was found to be 1054 mV. The temperature was maintained at 25°C throughout the operation. This sample electrode preparation process is shown in Fig. 2, and the layer formed was identified as $\beta\text{-PbO}_2$ by XRD analysis (Fig. 3).



All potentials mentioned here were referred to $\text{Hg}/\text{Hg}_2\text{SO}_4$ reference electrode.

Fig. 2. Sample electrode preparation process, and operation process of continuous EC-AFM observation.

2.3. AFM observation of the lead dioxide electrode

The electrochemical reaction of the lead dioxide electrode with sulfuric acid solution was observed under oxidation and reduction potentials, which was corresponding to the charge and discharge reactions of the positive electrode in a lead-acid battery. The in situ surface morphology change was observed by AFM when the potential was changed as follows. At first, two AFM images were observed while the potential was kept at 1250 mV for 10 min. Next, one AFM image was observed while the potential was changed from 1250 to 950 mV. And then, 11 AFM images were observed in the reduction potential at 950 mV for 10 min. Lastly, oxidation at 1250 mV for 10 min was applied again, during which 6 AFM images of the electrode were observed. During the observation of the 20 AFM images, the reduction or oxidation transient was measured. The observation time of an AFM image was 52 s, and the observation area was $5 \mu\text{m} \times 5 \mu\text{m}$. The temperature was maintained at 25°C . This operation process is also shown in Fig. 2.

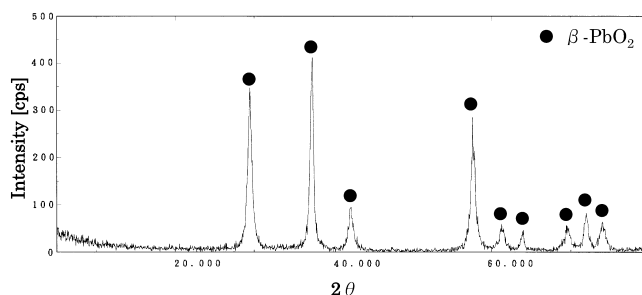


Fig. 3. X-ray diffraction pattern of the layer formed on the sample.

3. Results and discussion

3.1. Current transition obtained during the oxidation/reduction cycle

Fig. 4 shows the current transition observed with the potential change during the EC-AFM experiment. An oxidation potential of 1250 mV was applied to the lead dioxide electrode for 10 min in the first period of this experiment. Then the electrode was reduced at 950 mV for the next 10 min, and the potential was changed again to 1250 mV and maintained for 10 min. These potential operations to the lead dioxide electrode correspond to the charge, discharge and recharge of the positive electrode of a lead-acid battery, respectively.

During the first oxidation period, little oxidation current flowed to the electrode. This indicates that enough lead dioxide layer was formed in the previous preparation process, which covered the lead substrate completely. A sharp current peak was detected when reduction potential was applied and a broad current curve was observed when oxidation potential was applied again. Detailed explanation of these current peaks is made with AFM images later.

The AFM observations were carried out in this experiment during the periods A–E shown in Fig. 4. The length of the periods A, B and C corresponded to the observation time of an AFM image, and the continuous 11 images and six images were obtained during the terms of D and E, respectively.

3.2. AFM image of the lead dioxide electrode

Fig. 5 shows two morphology images of an electrode surface observed by AFM in 1.250 g/cm³ sulfuric acid during the first oxidation. Fig. 5a and b are the AFM images at the same point on the electrode indicated at periods A and

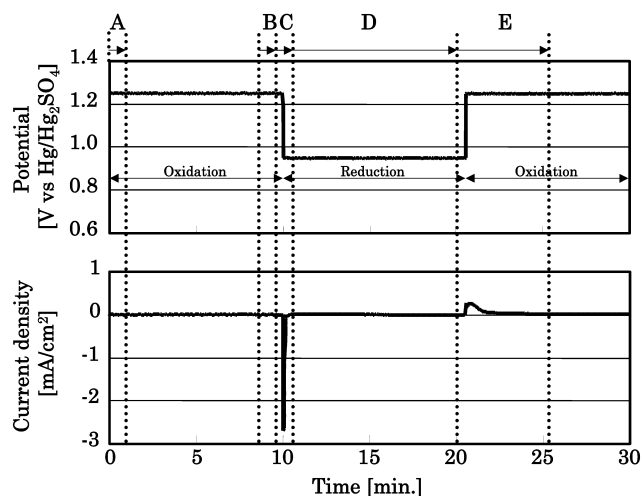


Fig. 4. Current transition and operated potential.

B in Fig. 4, respectively. As described above, these images are of the lead dioxide surface in sulfuric acid.

The AFM obtains a morphological image with the principle that a micro probe scans and measures the roughness of the sample surface. Therefore, it was previously considered that AFM observation of a lead dioxide surface might not be possible, because lead dioxide has rougher surface than a lead. However, it was confirmed in this experiment that observation of lead dioxide surface is possible in sulfuric acid as shown in Fig. 5.

There were no changes between Fig. 5a and b, and stable AFM images of lead dioxide surface were observed in the electrolyte under the charge condition. The electrode surface is composed of aggregates of small globular crystals, which are $\sim 0.2\text{--}0.5\ \mu\text{m}$ in diameter. For comparison, a SEM image of the positive active material of a lead-acid battery is shown in Fig. 6. Comparing the AFM and SEM images, it was confirmed that the morphology of the lead dioxide in this

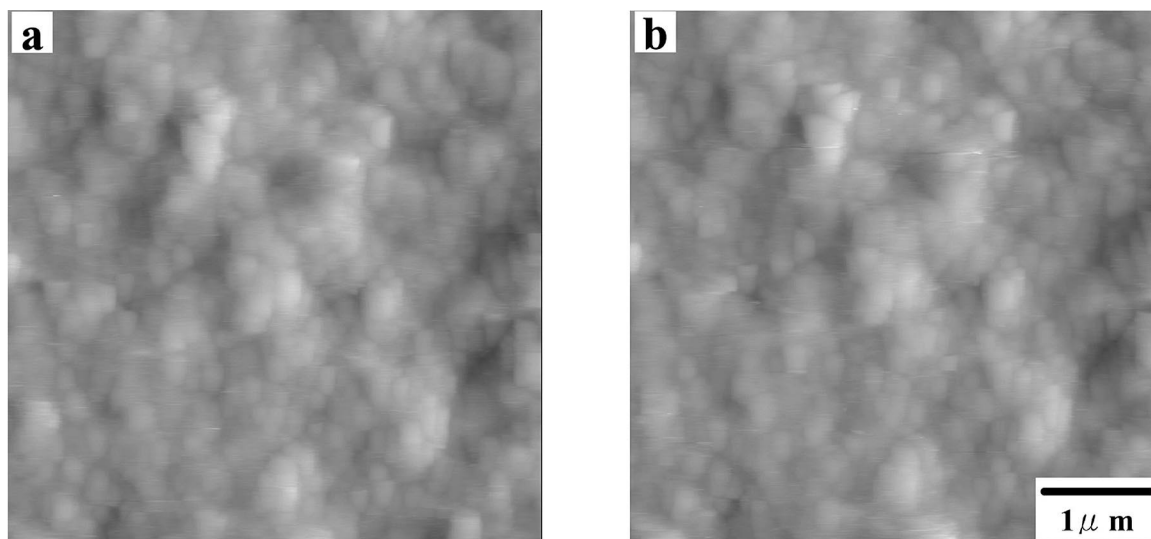


Fig. 5. AFM images of the lead dioxide electrode in sulfuric acid at 1250 mV vs. $\text{Hg}/\text{Hg}_2\text{SO}_4$: image a and b correspond to the period A and B in Fig. 4.

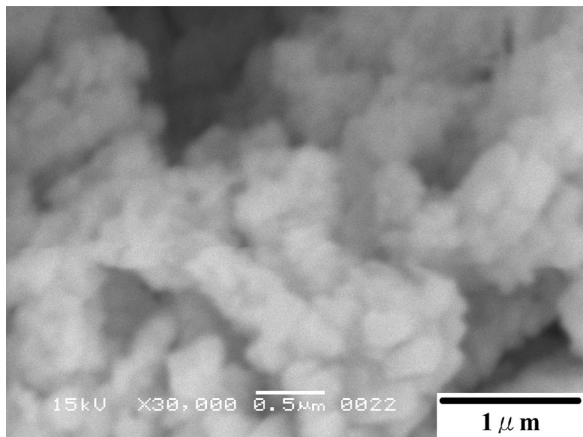


Fig. 6. SEM image of the positive active material of a lead-acid battery.

experiment was similar to that of the positive active material of the battery. Therefore, the prepared electrode was assumed to be a suitable model of the positive electrode, and so was used in the next electrochemical examination.

3.3. Morphology change of the lead dioxide electrode during oxidation/reduction cycle

AFM images of the electrode during oxidation/reduction cycle are shown in Figs. 7–9, which correspond to the observed images at the periods C–E shown in Fig. 4, respectively.

Fig. 7 shows an AFM image when the applied potential was changed from oxidation (1250 mV) to reduction (950 mV), with the current transient shown in a large scale at the right

side of the image. The image scan was made from bottom to the top of the image. A narrow horizontal line in Fig. 7 represents the potential change point, and the part under the line was the oxidation condition and the part over the line was the reduction condition in this figure. From this, it was found that the lead sulfate crystals were little formed until the reduction current reached the maximum of the peak, after which many crystals began to deposit. This result is similar to that found in the AFM study on the lead electrode [3,4], and can be understood as an indication that the reaction is composed of two step processes, the dissolution process of the lead dioxide electrode and the deposition process of the lead sulfate crystals after super-saturation of the electrolyte with lead ions.

Fig. 8 shows every second AFM image, from the sequence taken, during the reduction period. These images clearly show the morphology and sizes of the lead sulfate crystals formed by the reduction. These sizes were $\sim 0.3\text{--}1\ \mu\text{m}$ in this experimental condition, and they were larger than the lead dioxide crystals. From these images, it is noted that some crystals gradually grow during reduction. This behavior implies that the lead dioxide was discharged slowly when the electrode was kept in the reduction potential during these observations.

Fig. 9 shows the continuous images and the oxidation transient corresponding to period E in Fig. 4. The time regions I–VI indicated in the transient data correspond to the AFM images I–VI, respectively. White arrow in the images means the scanning direction of each AFM observation. A horizontal line in image I describes the potential change timing of 950–1250 mV: the part under the line was the reduction condition and the part over the line was the oxidation condition.

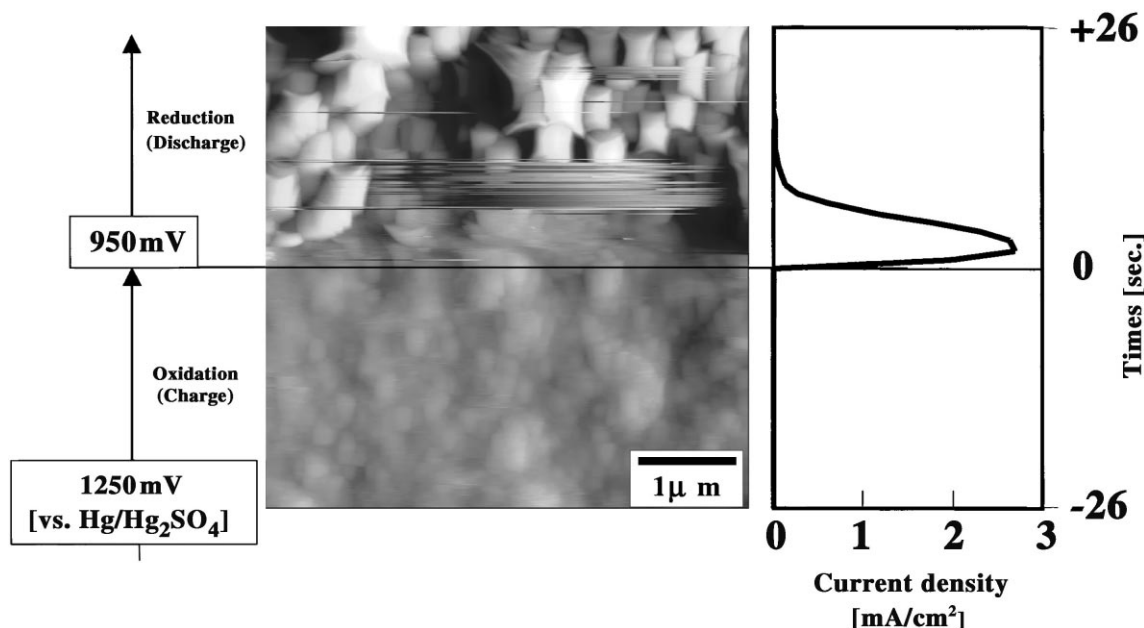


Fig. 7. AFM image of the lead dioxide electrode and reduction current transient with potential change; applied potential was changed from 1250 to 950 mV at the horizontal line.

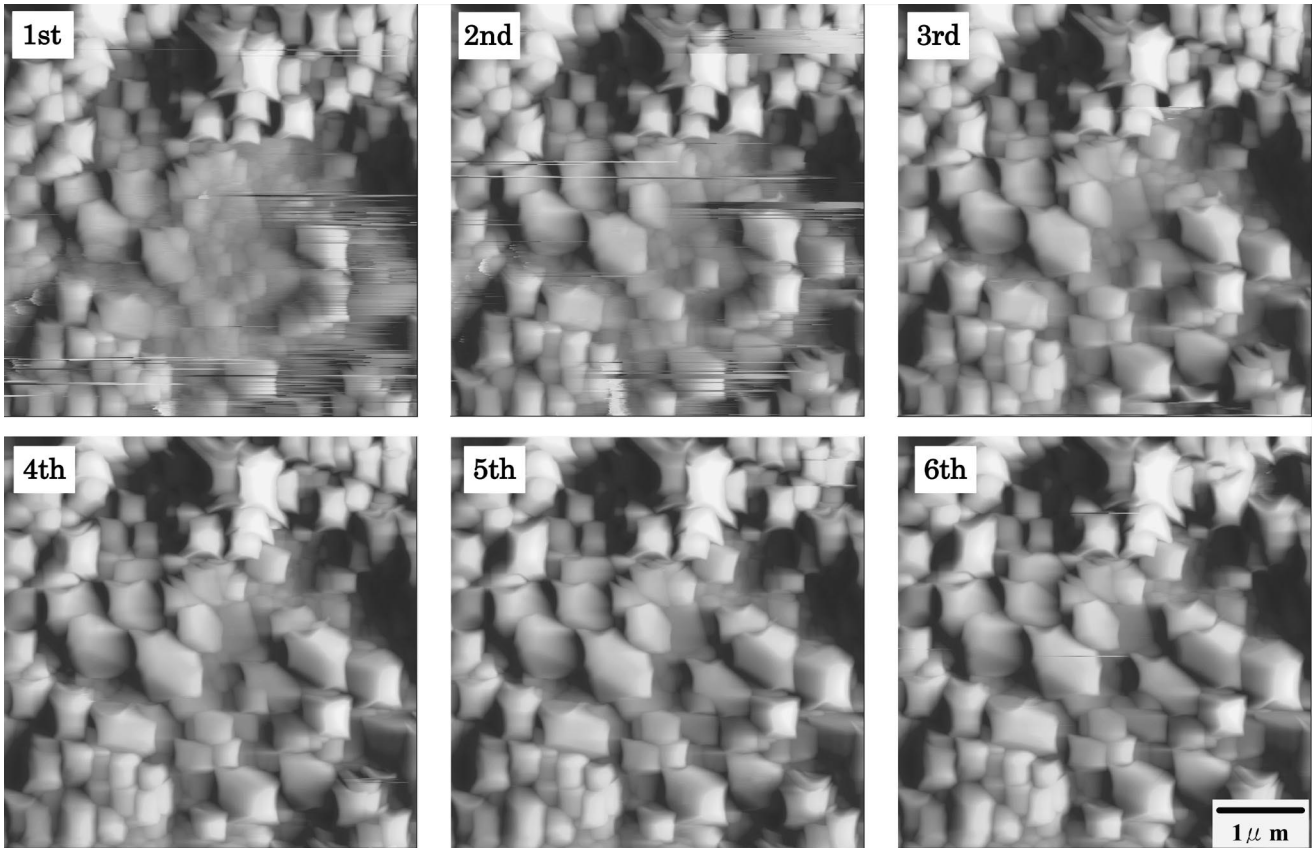


Fig. 8. AFM images of the lead dioxide electrode at the reduction potential, 950 mV vs. Hg/Hg₂SO₄.

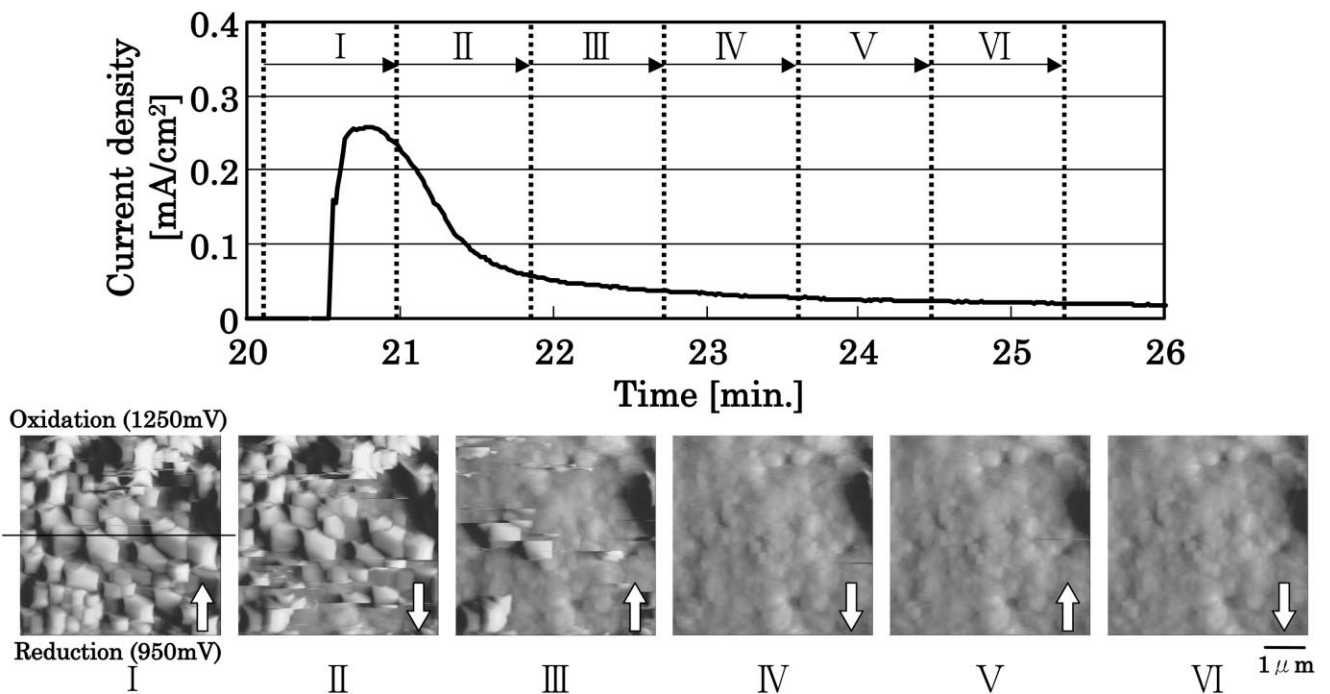


Fig. 9. Continuous AFM image of the lead dioxide electrode and oxidation current transient; the applied potential was changed from 950 to 1250 mV at the horizontal line in the image I. The arrow in the figures indicates the measurement direction.

It can be seen from the region/image I in Fig. 9 that the oxidation current was detected from the moment that the oxidation potential was applied at the horizontal line, but the formed lead sulfate crystals hardly dissolved for about 30 s after the potential change. This oxidation behavior was obviously different from the reduction behavior shown in Fig. 7. Two reasons are considered for this in dissolution of the crystals. One reason is the capacitance effect. Because the current is only used to charge the capacitance of the electrode, it does not resolve the lead sulfate. The other is the internal reaction process. The AFM can obtain only surface information of the sample, therefore, it cannot capture the reaction if dissolution of the lead sulfate occurs from the internal side of the electrode.

It was understood from the continuous AFM images that the dissolution of whole crystals took ~ 2 min, and the oxidation transient was recorded as a broad curve with its maximum current being much smaller than the reduction one. These results suggest that the oxidation is slower than the reduction, indicating that the charge reaction of the positive electrode has to be studied in detail as well as that of the negative electrode in order to improve the charge acceptability of the lead-acid battery for EV and HEV applications.

4. Conclusions

We succeeded in direct observation of morphology change of a lead dioxide electrode during oxidation/reduction cycle by using EC-AFM. The experimental results led to the following conclusions.

1. The in situ EC-AFM is a useful technique for observation of the behavior of the lead dioxide electrode during the oxidation/reduction cycle.

2. The reduction of a lead dioxide electrode is composed of two step processes, which are the dissolution process of the lead dioxide electrode and the deposition process of lead sulfate crystals after saturation of electrolyte with lead ions.
3. Lead sulfate crystals formed by reduction are gradually dissolved at the oxidation potential, and this reaction is obviously slower than the reduction of the lead dioxide electrode.

We believe that the function of the positive electrode of the lead-acid battery is further clarified by the application of this EC-AFM technique.

References

- [1] Y. Yamaguchi, M. Shiota, Y. Nakayama, N. Hirai, S. Hara, *J. Power Sources* 85 (2000) 22–28.
- [2] Y. Yamaguchi, Y. Nakayama, N. Hirai, S. Hara, *YUASA-JIHO* 85 (1998) 6–11.
- [3] Y. Yamaguchi, M. Shiota, Y. Nakayama, N. Hirai, S. Hara, *J. Power Sources* 93 (1–2) (2001) 104–112.
- [4] Y. Yamaguchi, M. Shiota, Y. Nakayama, N. Hirai, S. Hara, *YUASA-JIHO* 89 (2000) 29–37.
- [5] D. Pavlov, *J. Power Sources* 42 (1993) 345–363.
- [6] Y. Nakayama, T. Takayama, M. Kono, *YUASA-JIHO* 53 (1982) 56–66.
- [7] D. Pavlov, *J. Power Sources* 33 (1991) 221–229.
- [8] B. Culpin, A.F. Hollenkamp, D.A.J. Rand, *J. Power Sources* 38 (1992) 63–74.
- [9] J. Yamashita, M. Yamane, M. Kono, *YUASA-JIHO* 49 (1980) 17–24.
- [10] A. Kita, Y. Matsumaru, J. Yamashita, *YUASA-JIHO* 58 (1985) 7–14.
- [11] Y. Nakayama, Y. Sasaki, M. Kono, *YUASA-JIHO* 47 (1979) 30–37.